# Relativistic Laboratory Astrophysics with Relativistic Laser Plasmas


**S. V. Bulanov**

*Advanced Photon Research Center,*
*Japan Atomic Energy Agency, Kizugawa-shi, Kyoto-fu, Japan*
*A. M. Prokhorov Institute of General Physics, RAN, Moscow, Russia*



**$4^{th}$ International Sakharov Conference on Physics**
**May 17-23, Moscow, Russia**




**3D PIC & EXPERIMENT**

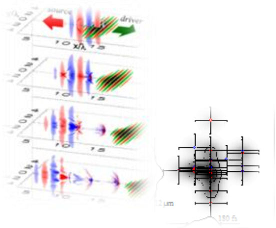


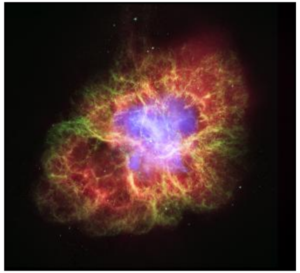

# Acknowledgments


M. Borghesi
T. Zh. Esirkepov
D. Habs
I. N. Inovenkov

M. Kando
F. Pegoraro
A. S. Pirozhkov
T. Tajima

# OUTLINE

1. Lasers and Astrophysics
2. Shock Waves
3. Reconnection of Magnetic Field Lines & Vortex Patterns
4. Relativistic Rotator
5. Flying Mirror for Femto-, Atto-, … Super Strong Fields
6. Overdense Accelerating Mirror (KAGAMI)
7. Applications
8. Conclusion

# 1. Lasers and Astrophysics

## Morphology of Entities in Space and Laser Plasmas

NIF

HiPER

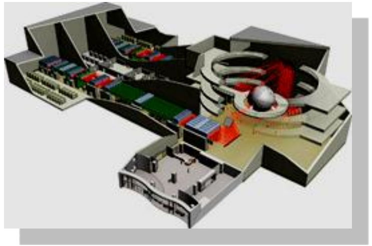

ELI

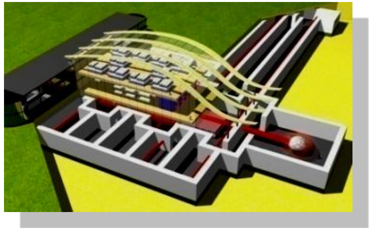

### Wake

The Mouse Pulsar

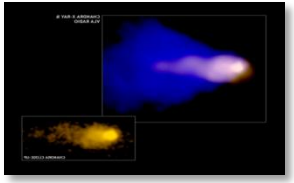

Electron Wake

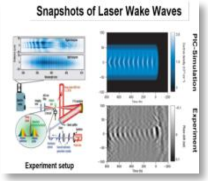


Matlis et al, (2006)

Ion Wake

experiment

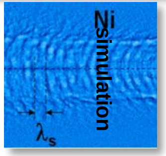


Borghesi, et al, (2005)

### Bow Wave

Chandra image of M87

Electron Bow Wave

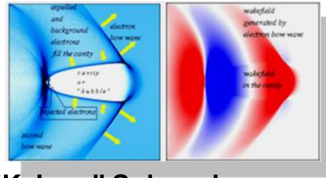

Esirkepov et al (2008)

"Kalmar" Submarine

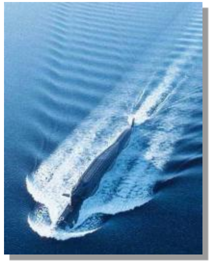

### Photon Bubbles

"Black Widow" pulsar

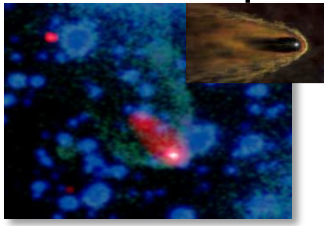

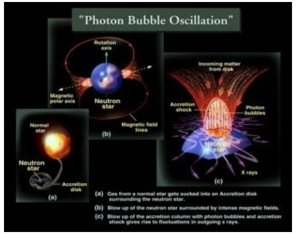


RPDA

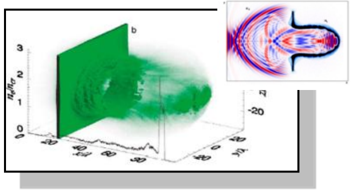

Esirkepov et al (2004)

# Relativistic Limit in EM Wave – Plasma Interaction

Quiver energy of electron oscillating in the EM wave with the amplitude $E_0$ and frequency $\omega$ becomes larger than $m_e c^2$ when the dimensionless amplitude of the EM wave is greater than unity:

$$a_0 = \frac{eE_0}{m_e \omega c} > 1$$

In the EM wave interaction with the electron in vacuum its electron energy scales as (Landau & Lifshitz)

$$\mathcal{E} = \frac{1}{2} m_e c^2 a_0^2$$

When the electron oscillates in the EM wave propagating in a plasma we have (Akhiezer & Polovin)

$$\mathcal{E} = m_e c^2 a_0$$

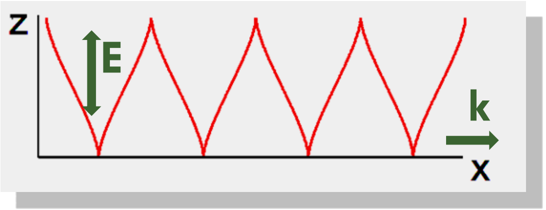


Laser: Condition $a_0 > 1$ corresponds for 1μm laser wavelength to the intensity above $1.35 \times 10^{18}$ W/cm$^2$

Today's lasers can provide the intensity $I > 2 \times 10^{22}$ W/cm$^2$, i. e. $a_0 \approx 100$

**V.Yanovskij et al (2008)**

# Magneto-dipole Radiation of Oblique Rotator

**Space:** Magneto-dipole radiation of oblique rotator, has been considered as a model for the pulsar radiation

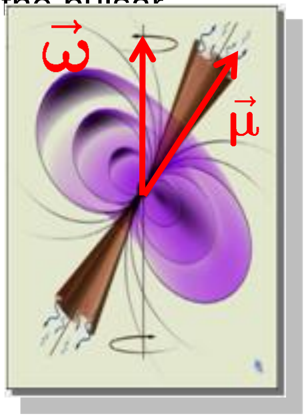


$r = \frac{c}{\omega}$

(Michel;
Beskin, Gurevich, Istomin)

Power emitted by rotator is given by $W = \frac{2}{3}\frac{\mu^2 \sin\theta^2 \omega^4}{c^3}$

Magnetic moment: $\mu \approx B r_p^3$ ; $\theta$ is the angle between $\vec{\mu}$ and $\vec{\omega}$

The EM wave intensity at the distance r is $I = W / 4\pi r^2$

In the wave zone, $r = c/\omega$ , the dimensionless wave amplitude is

$$a_0 = \frac{e\mu\omega^2}{m_e c^4}$$

For typical values of magnetic field, $B = 10^{12} G$ , rotation frequency , $\omega = 200 s^{-1}$,

and pulsar radius: $r_p = 10^6 cm$

it yields $a_0 = 10^{10}$

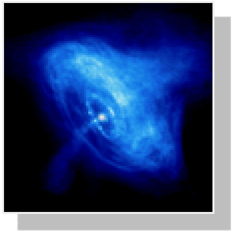

Crab pulsar

| Amplitude $\left[a_0 = \frac{eE_0}{m_e c\omega}\right]$ | Intensity $\left[\frac{\text{W}}{\text{cm}^2}\right]$ | Regime |
|---|---|---|
| $a_{QED} = \frac{m_e c^2}{h\omega}$ | $2.4 \times 10^{29}$ | $e^+, e^-$ in vacuum |
| $a_{QM} = \frac{2e^2 m_e c}{3h^2\omega}$ | $5.6 \times 10^{24}$ | quantum effects |
| $a_p = \frac{m_p}{m_e}$ | $1.3 \times 10^{24}$ | relativistic p |
| $a_{rad} = \left(\frac{3\lambda}{4\pi r_e}\right)^{1/3}$ | $1 \times 10^{23}$ | radiation damping |
| $a_{rel} = 1$ | $1.3 \times 10^{18}$ | relativistic $e^-$ |

A. Illarionov & Ya. B. Zel'dovich, 1975; A.G.Zhidkov, et al., 2003
SVB, T. Zh. Esirkepov, J. Koga, T. Tajima, 2004

Cross section of nonlinear Thomson scattering

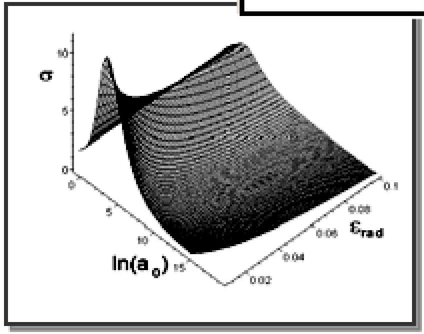


For the Crab pulsar,

$\omega = 200\,s^{-1}, \quad a_0 = 10^{10}$

the radiation damping effects are crucially important because the EM wave amplitude is above the threshold:

$$a_{rad} = \left(\frac{3\lambda}{4\pi r_e}\right)^{1/3} = 10^7$$

# Laser-Plasma Interaction in the "Radiation-Dominant" Regime

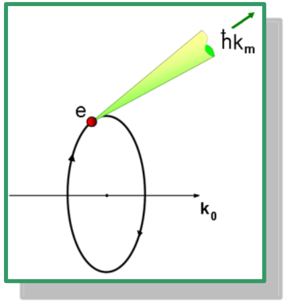


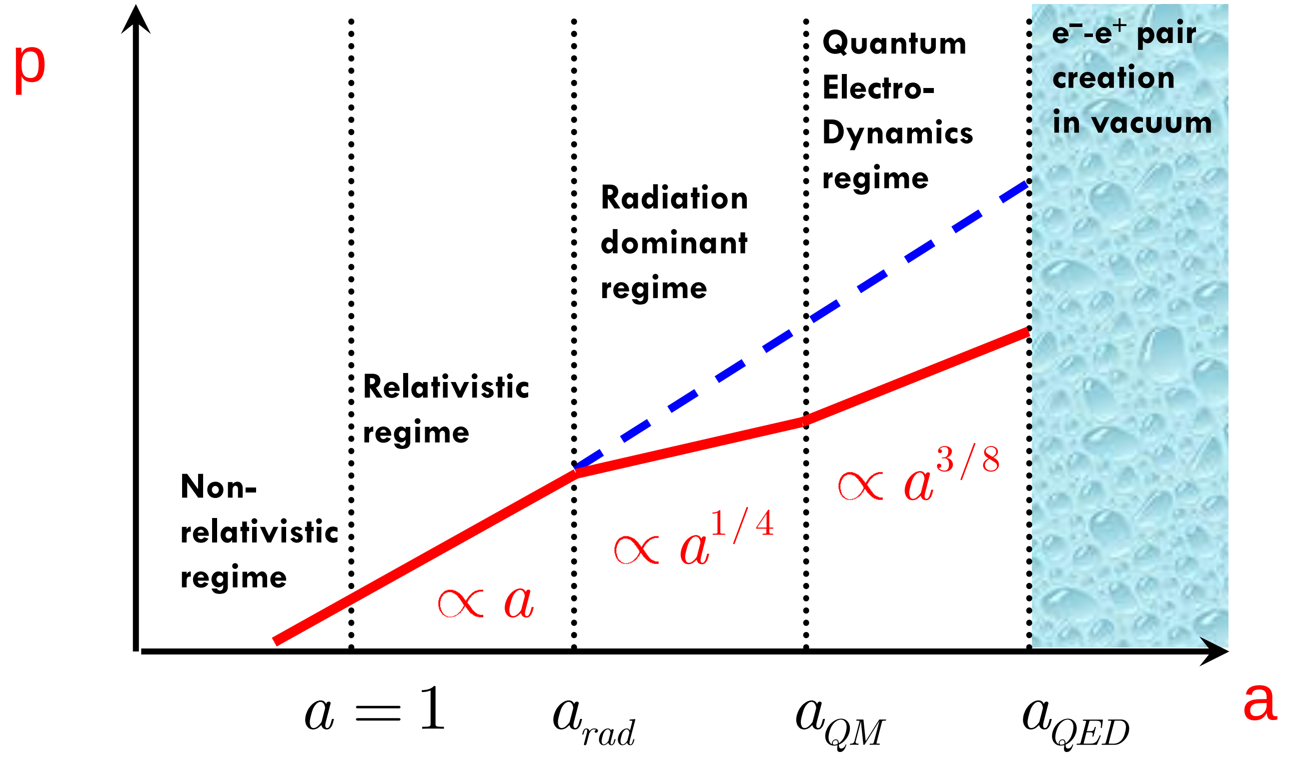

# Laboratory Astrophysics

## Laboratory Astrophysics

**Relativistic Laboratory Astrophysics with the Ultra Short Pulse High Power Lasers**

**We deal with the collisionless plasmas**

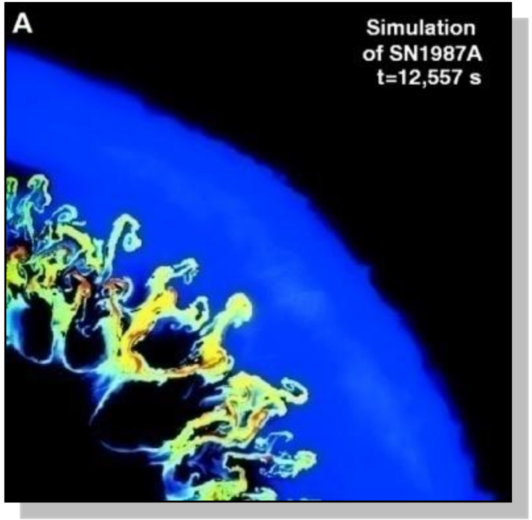


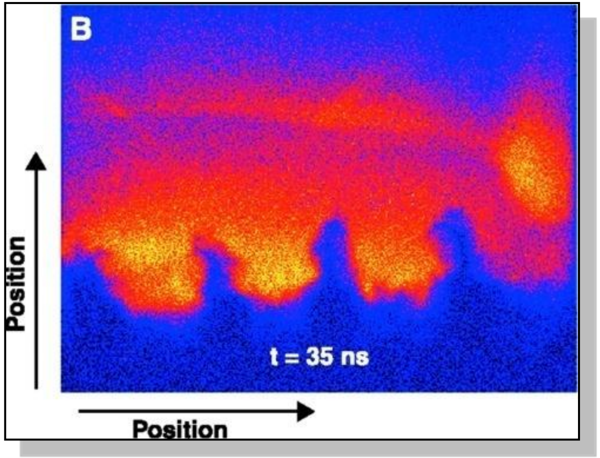


B. A. Remington et al., Science 284, 1488 (1999)

*Rayleigh-Taylor & Richtmayer-Meshkov Instability,:*
*seen in simulations of Supernovae (right) and*
*in laser irradiated Nuclear Fusion target*

*Radiative shock waves, plasma jets*

# Plasma jets driven by Ultra-intense laser interaction with thin foils

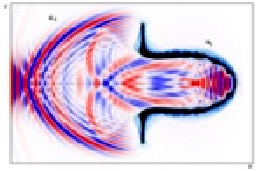

VULCAN Nd-glass laser of Rutherford Appleton laboratory,
(60 J, 1ps & 250 J, 0.7 ps) interacts with foils (3, 5 mum, Al & Cu)

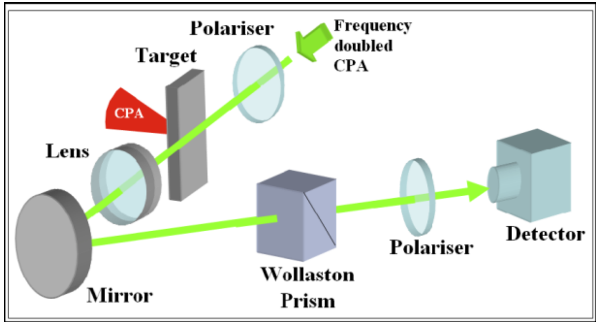


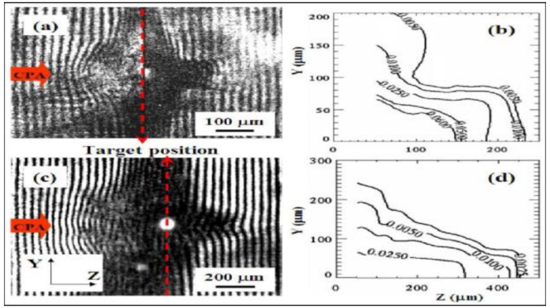


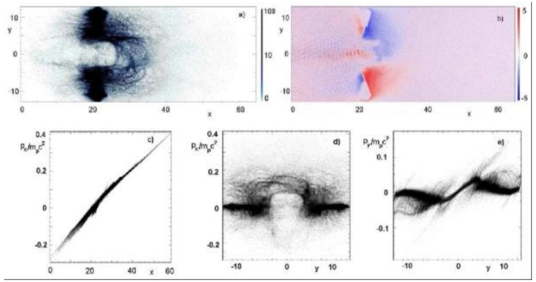

$$\frac{p^{(0)}}{m_p c} = \frac{2W(W+1)}{2W+1} \approx 2W$$

$$W = \int \frac{E^2(\psi)}{2\pi n_0 l} d\psi \ll 1$$

S. Kar, M. Borghesi, SVB, A.J. Mackinnon, P.K. Patel,
M.H. Key, L. Romagnani, A. Schiavi, A. Macchi, and O. Willi , PRL (2008)

# Reconnection of Magnetic Field Lines

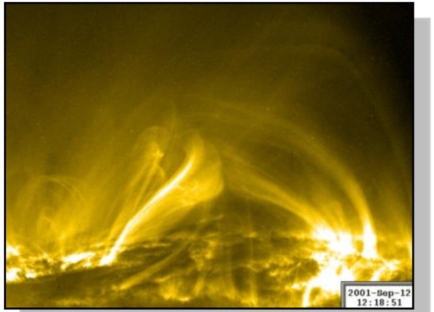


Solar flare/
12.09.2001(12:18:51)

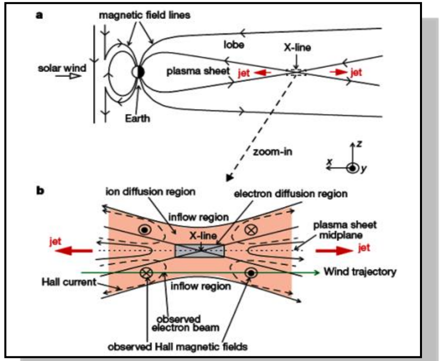


M. Oieroset, et al.,
Nature (2001)

B.Coppi et al (1965)

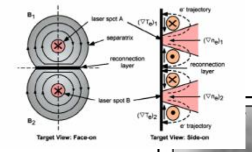


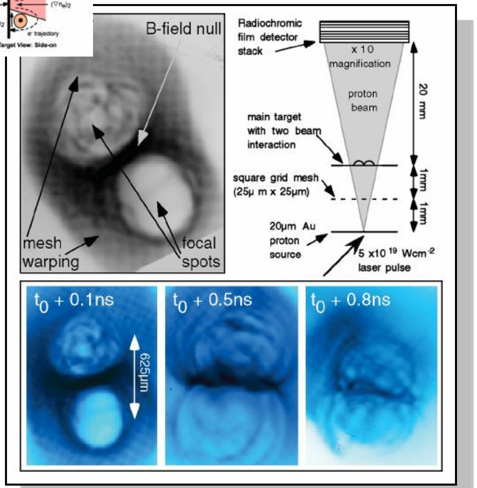


Nilson et al, PRL 97, 255001 (2006)

**MAGNETIC RECONNECTION IN LASER PLASMAS HAS BEEN FORESEEN IN:**

G.A.Askar'yan, SVB, F.Pegoraro, A.M.Pukhov,
Magnetic interaction of self-focused channels and magnetic wake excitation in high intense laser pulses,
Comments on Plasma Physics and Controlled Fusion 17, 35 (1995).

# 2. Shock Waves

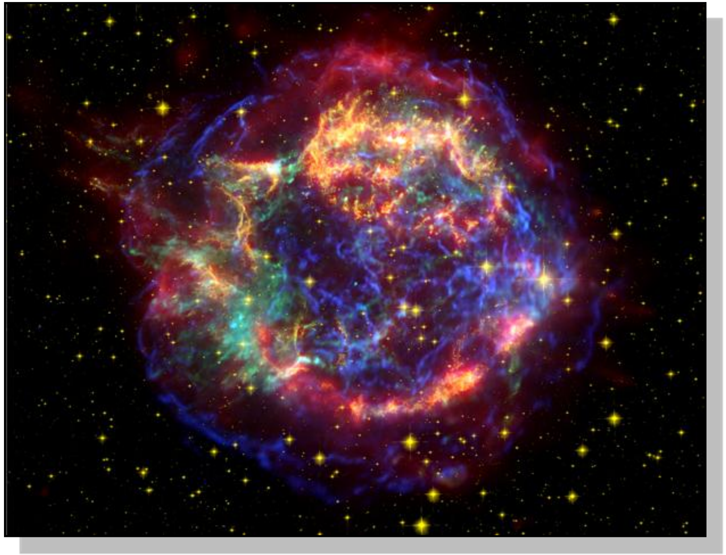

Cassiopea A

# Shock Waves and RT Instability

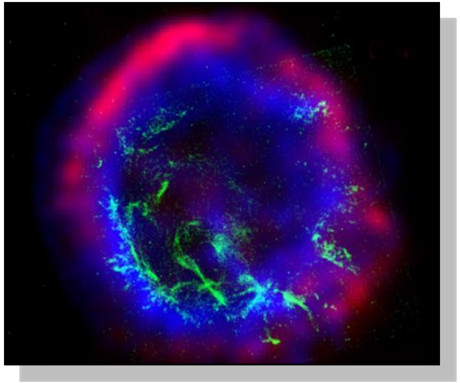

Supernova Remnant
E0102-72
from Radio to X-Ray

SNII $\mathcal{E}_{tot} = 10^{52} erg$

$1/10 \quad - \quad 1/30 \quad year$

$2\% \quad - \quad 10\%$

**TeV gamma sources**

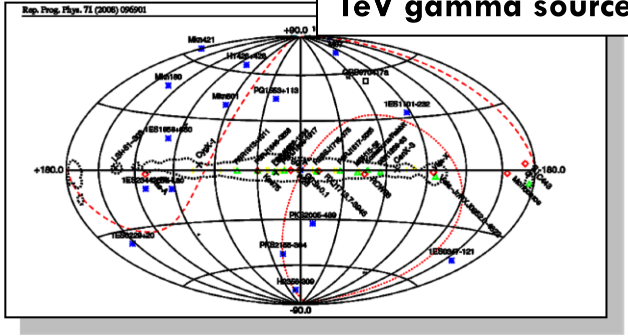


Shock Wave

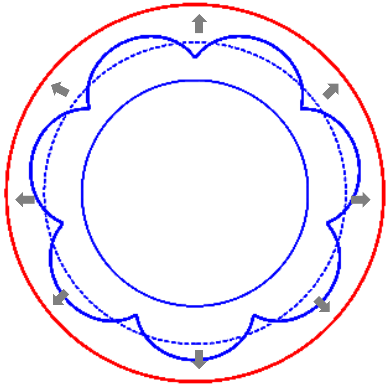

Rayleigh – Taylor
&
Richtmayer-
Meshkov
instabilities

1. Ballistic motion of the ejecta

2. Sedov's regime:

$$R_{SW} = 1.5(\mathcal{E}_{tot} t^2 / \rho)^{1/3} = \frac{5}{2} V_{SW} t$$

$$V_{SW} \propto t^{-3/5}$$

3. Radiation losses: $R_{SW} \propto t^{2/7}$

# Acceleration at the Shock Wave Front

**CR have a power law energy spectrum over several orders of magnitude energy range**

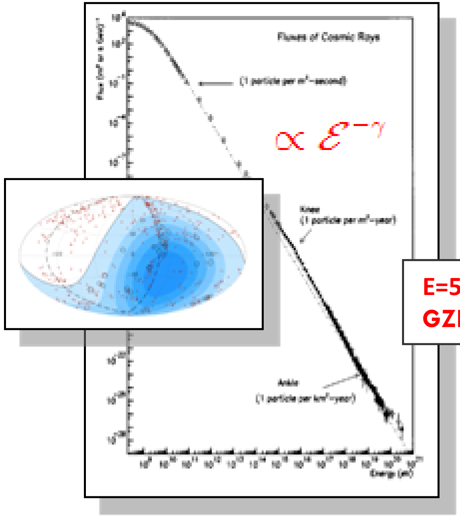


**$E=5 \times 10^{19}$ eV**
**GZK-cutoff**

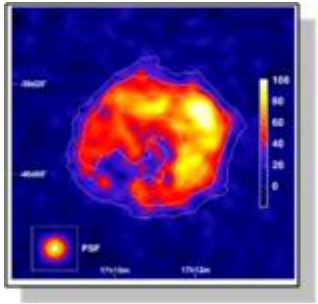

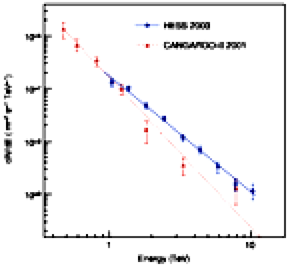

**The gamma ray image of RX J1713.7-3946 spectrum and gamma ray obtained with the HESS telescope array (Aharonyan et al, 2008)**

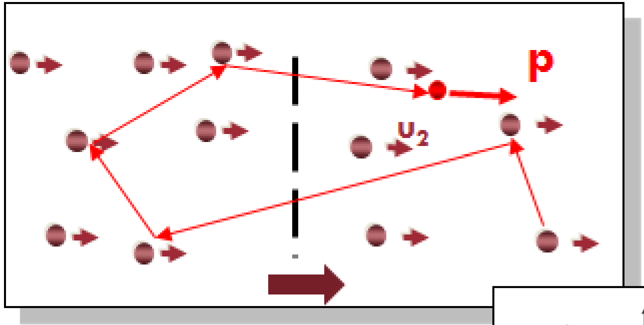


**"Fermi acceleration"**
G.F. Krymskii (1977)

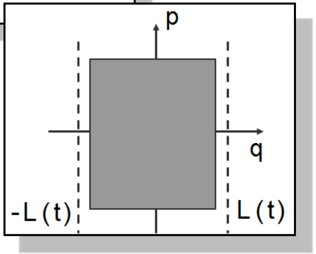


$$\frac{\partial}{\partial x}\left(u(x)f - D\frac{\partial f}{\partial x}\right) = -\frac{2u_1}{3(\kappa+1)}\delta(x)\frac{1}{p^2}\frac{\partial}{\partial p}\left(p^2 f\right)$$

$$pL = const$$

$$u_2 = \frac{\kappa-1}{\kappa+1}u_1 \qquad u_1 > u_2$$

$$f(p) = Cp^{-\gamma}$$

$$\gamma = \frac{3u_1}{u_1 - u_2}$$

# Collisionless Shock Waves

A structure of collisionless schock waves is determined by the counter play of dissipation and dispersion effects. These effects are described within the framework of the Korteweg-de Veries-Burgers equation:

$$\partial_t u + u\partial_x u - \nu\,\partial_{xx} u - \beta\,\partial_{xxx} u = 0$$

nonlinearity dispersion

dissipation

R.Z.Sagdeev, 1959

a) MS wave propagating almost perpendicularly to B field $\beta \approx v_a c^2 / 2\omega_{pe}$

with $v_a = B^2 / \sqrt{4\pi n m_p}$

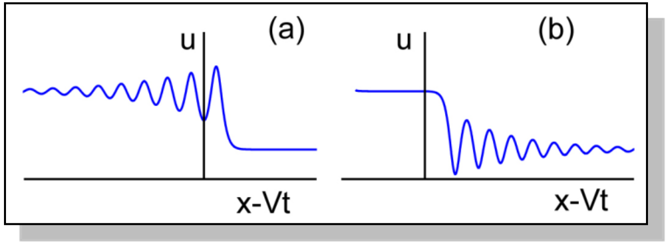


b) MS wave propagation is almost parallel to B field

$$\beta \approx -v_a c^2 / 2\omega_{pe}$$

# Observation of Collisionless Shocks in Laser-Plasma Experiments

L. Romagnani,[1,*] S. V. Bulanov,[2,3] M. Borghesi,[1] P. Audebert,[4] J. C. Gauthier,[5] K. Löwenbrück,[6] A. J. Mackinnon,[7] P. Patel,[7] G. Pretzler,[6] T. Toncian,[6] and O. Willi[6]
[1]School of Mathematics and Physics, The Queen's University of Belfast, Belfast, Northern Ireland, United Kingdom
[2]APRC, JAEA, Kizugawa, Kyoto, 619-0215 Japan
[3]Prokhorov Institute of General Physics RAS, Moscow, 119991 Russia
[4]Laboratoire pour l'Utilisation des Lasers Intenses (LULI), UMR 7605 CNRS-CEA-École Polytechnique-Univ, Paris VI, 91128 Palaiseau, France
[5]Université Bordeaux 1; CNRS; CEA, Centre Lasers Intenses et Applications, 33405 Talence, France
[6]Institut für Laser–und Plasmaphysik, Heinrich-Heine-Universität, Düsseldorf, Germany
[7]Lawrence Livermore National Laboratory, Livermore, California 94550, USA
(Received 4 April 2008; published 10 July 2008)

The propagation in a rarefied plasma ($n_e \lesssim 10^{15}$ cm$^{-3}$) of collisionless shock waves and ion-acoustic solitons, excited following the interaction of a long ($\tau_L \sim 470$ ps) and intense ($I \sim 10^{15}$ W cm$^{-2}$) laser pulse with solid targets, has been investigated via proton probing techniques. The shocks' structures and related electric field distributions were reconstructed with high spatial and temporal resolution. The experimental results were interpreted within the framework of the nonlinear wave description based on the Korteweg–de Vries–Burgers equation.

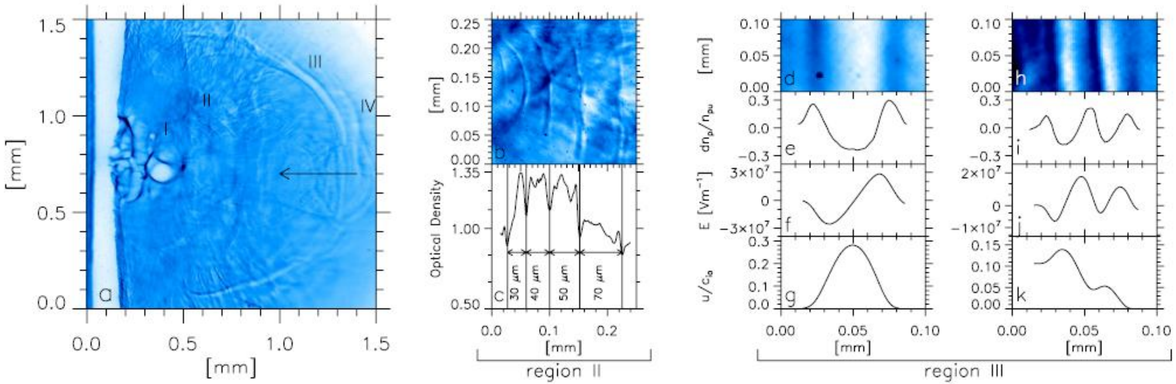


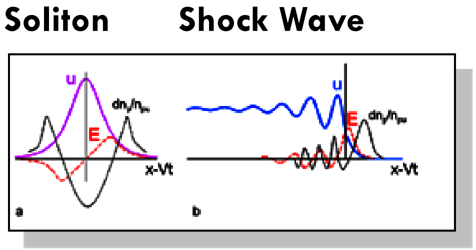

# 3. Reconnection of Magnetic Field Lines & Vortex Patterns

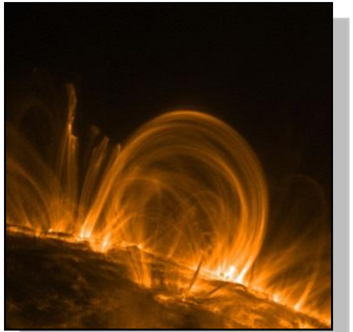

Solar Flare

Von Karman vortex row made by the wind over the Pacific island of Guadalupe

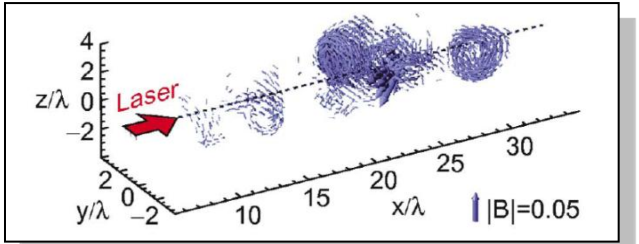


Magnetic (vortex) wake behind the laser pulse: Esirkepov, et al., 2004

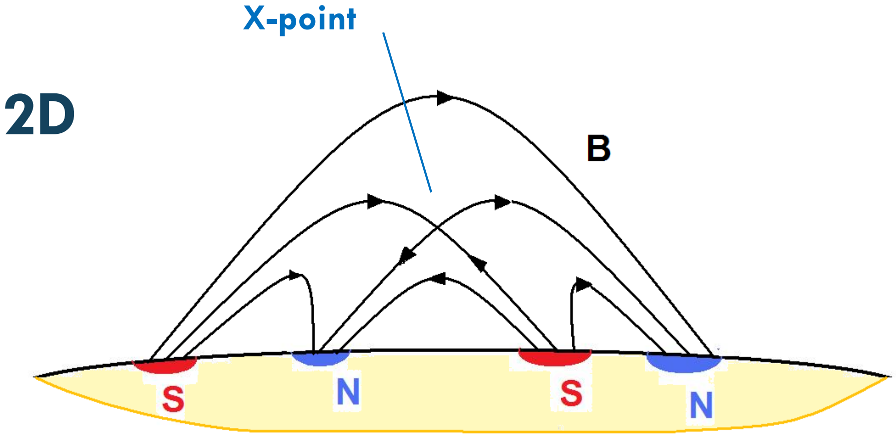


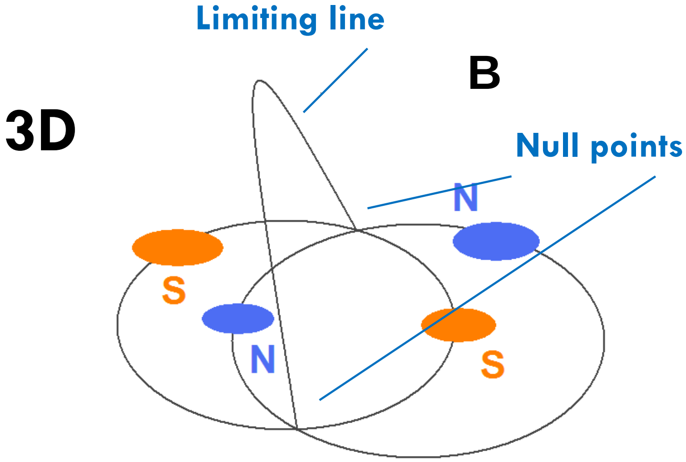


Sweet (1965)

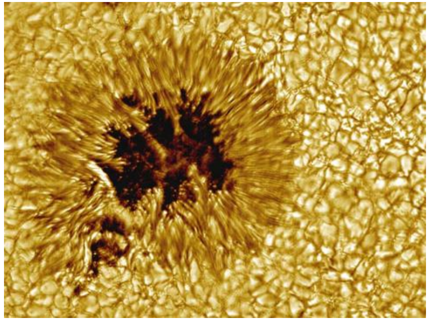

Sunspot

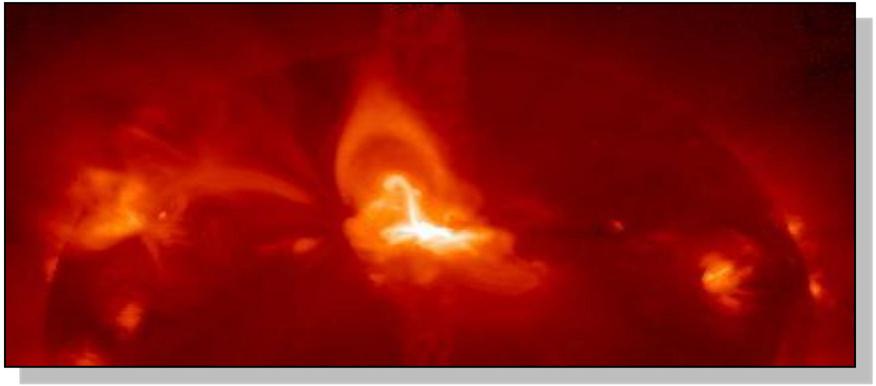

Solar Flare

**2D case:** The field-line equation reads

$$\frac{dx}{B_x} = \frac{dy}{B_y} = ds$$

Using the relationships

$$B_x = \partial_y A_z - \partial_x F, \quad B_y = -\partial_x A_z - \partial_y F,$$

introducing complex variable $\varsigma = x + iy$, complex field and potential

$$B = B_x - iyB_y, \quad \Phi = F - iA_z,$$

we obtain the Hamiltonian equations for the magnetic field lines $(' = d/ds)$:

$$\varsigma' = -\frac{\partial \Phi}{\partial \varsigma}$$

The magnetic field lines are on the surfaces $A_z =$ constant

# Local Structure of the Magnetic Field

Near null point we can expand the magnetic field as

$$\mathbf{B}(\mathbf{x},t) = (\mathbf{B}(0,t)\nabla)\mathbf{x} + \ldots.$$

Introducing the matrix $\partial B_i / \partial x_j\big|_{x=0} = A_{ij}, \quad B_i = A_{ij} x_j$

we write for the magnetic field lines $\dfrac{dx_i}{ds} = A_{ij} x_j.$

It yields $\det \; A_{ij} - \lambda \delta_{ij} \; = 0,$

The topology is determined by the eigenvalues $\lambda_\alpha \quad \sum_\alpha \lambda_\alpha = 0$

We have the null surface, null line or null point depending on

$\lambda_{1,2} = \pm \lambda'$ or $\lambda_{1,2} = \pm i\lambda'' \quad \lambda_3 = 0$

$\lambda_{1,2} = \lambda' \pm i\lambda'' \quad \lambda_3 = \lambda'$

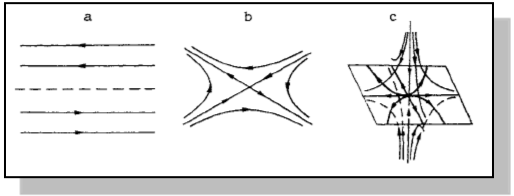


**SVB, M. A.Ol'shanetskij (1983)**

# MHD Equations

$$\partial_t \rho + \nabla(\rho \mathbf{v}) = 0,$$

$$\partial_t \mathbf{v} + (\mathbf{v}\nabla)\mathbf{v} = \frac{(\nabla \times \mathbf{B}) \times \mathbf{B}}{4\pi\rho},$$

$$\partial_t \mathbf{B} = \nabla \times (\mathbf{v} \times \mathbf{B}) + \nu_m \Delta \mathbf{B},$$

$$\nabla \cdot \mathbf{B} = 0$$

$\rho$ - plasma density; $\mathbf{v}$ - velocity; $\mathbf{B}$ - magnetic field; $\nu_m$- magnetic diffusivity

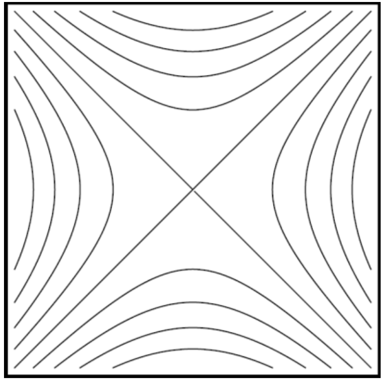

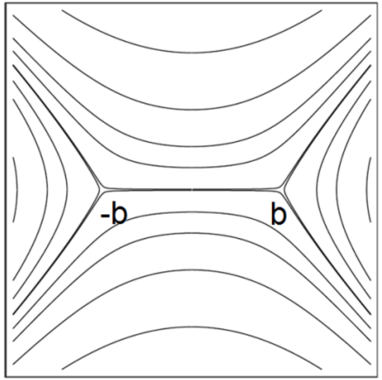


S. I. Syrovatskii, 1971

$$b = \sqrt{4I / hc}$$

$$\Phi = h\varsigma^2 / 2$$

$$\Phi = h\left[\varsigma\sqrt{\varsigma^2 - b^2} - \mathrm{Ln}\left(\varsigma - \sqrt{\varsigma^2 - b^2}\right)\right]$$

Current sheet near the X-line
of magnetic configuration

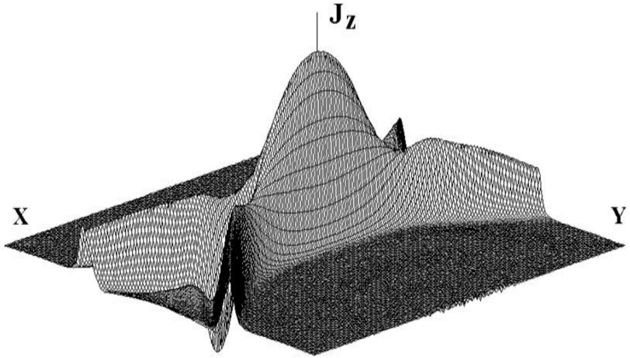


SVB, et al, 1996

# Magnetic Reconnection in Collisionless Plasmas

In collisionless multispecies plasmas the **curl** of the canonical momentum

$$\mathbf{p}_\alpha = m_\alpha \mathbf{v}_\alpha + (e_\alpha / c)\mathbf{A}$$

is frozen in the corresponding flow velocity

$$\partial_t \nabla \times \mathbf{p}_\alpha = \nabla \times \mathbf{v}_\alpha \times \nabla \times \mathbf{p}_\alpha$$

The electron magnetohydrodynamics considers the dynamics of just the electrons, the ions are assumed to be at rest and the quasineutrality condition is fulfilled. The electron velocity is related to the magnetic field as

$$\mathbf{v}_e = -(c / 4\pi n_e)\nabla \times \mathbf{B}$$

with constant plasma density $n_e = n_i$. It yields

$$\partial_\mathbf{t}(\mathbf{B} - \Delta\mathbf{B}) = \nabla \times [(\nabla \times \mathbf{B}) \times (\mathbf{B} - \Delta\mathbf{B})]$$

In the linear approximation EMHD describes the whistler waves

The EMHD equations can be written as

$$\partial_t \mathbf{\Omega} = \nabla \times [(\nabla \times \mathbf{B}) \times \mathbf{\Omega}]$$

Here the generalized vorticity

$$\mathbf{\Omega} = \mathbf{B} - \Delta\mathbf{B} = \nabla \times (\mathbf{A} - \Delta\mathbf{A}) = \mathbf{B} + \nabla \times \mathbf{v}$$

is frozen into the electron fluid motion.

We consider the magnetic field given by

$$\mathbf{B} = \nabla \times (A_{||}\mathbf{e}_z) + B_{||}\mathbf{e}_z$$

The magnetic field pattern in the $x, y$ plane is determined by

$$A_{||}(x, y, t) = const$$

## Magnetic field

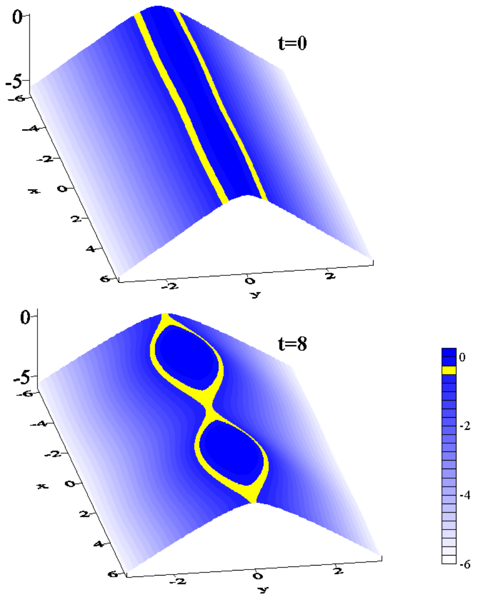


$$A_{||} = \text{const}$$

## Generalized vorticity

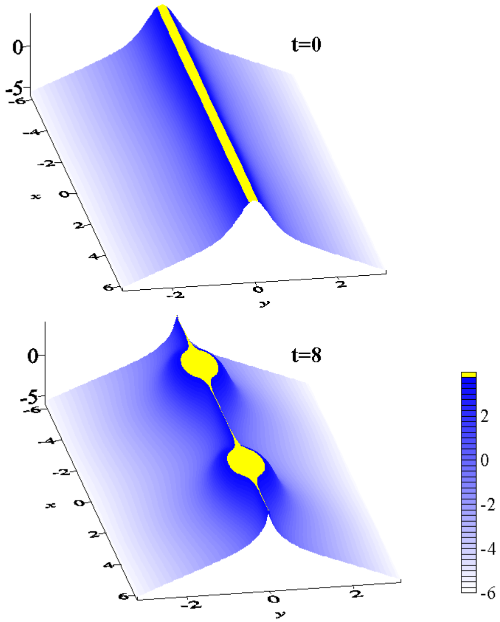


$$A_{||} - \Delta A_{||} = \text{const}$$

**K.Avinash, SVB, T.Esirkepov, P.Kaw, F.Pegoraro, P.Sasorov, A.Sen,**
**Forced Magnetic Field Line Reconnection in Electron Magnetohydrodynamics.**
***Physics of Plasmas* 5, 2946 (1998)**

# Charged Particle Acceleration

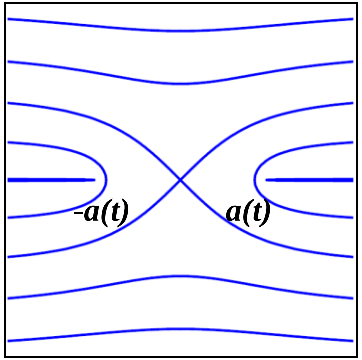


$$\Phi(\varsigma,t) = B_0\sqrt{a^2(t)-\varsigma^2}$$

In the vicinity of the X-line, the magnetic field is described by

$$B(\varsigma,t) = B_0\frac{\varsigma}{\sqrt{a^2(t)-\varsigma^2}} \approx B_0\frac{\varsigma}{a(t)}$$

and the electric field is given by

$$E(\varsigma,t) = -B_0\frac{a(t)\dot{a}(t)}{c\sqrt{a^2(t)-\varsigma^2}} \approx \frac{\dot{a}(t)}{c}B_0$$

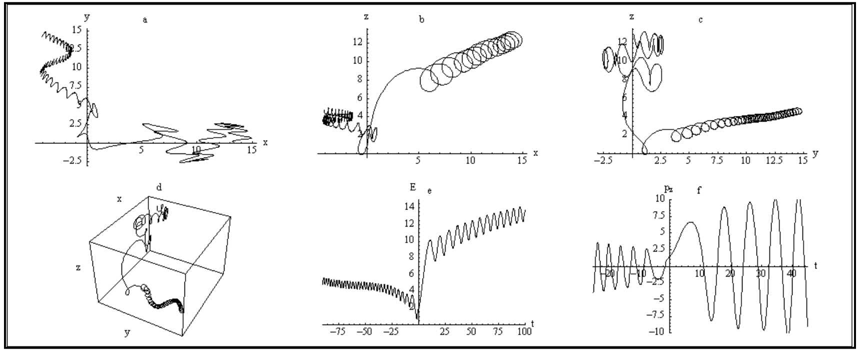


The energy spectrum of fast particles is given by

$$\frac{d\mathcal{N}(\mathcal{E})}{d\mathcal{E}} \propto \exp\left(-\sqrt{\frac{2\mathcal{E}}{m\dot{a}^2}}\right)$$

SVB, Sasorov; SVB, Cap

# Electron Vortices behind the Laser Pulse

Antisymmetric vortex row

$B_z(x, y)$

$n_i(x, y)$

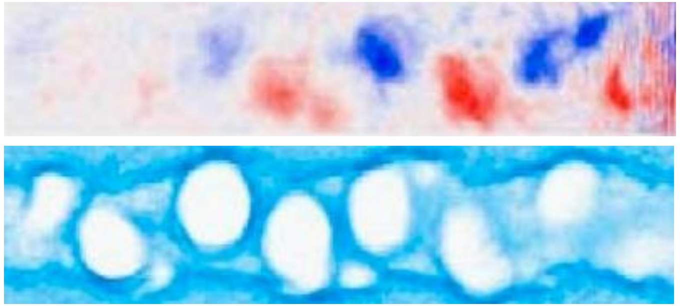

L.M.Chen et al., Phys. Plasmas, 14, 040703 (2007)

Von Karman vortex row
H.Lamb, Hydrodynamics, 1947

Vortices described by the Hasegawa-Mima equation

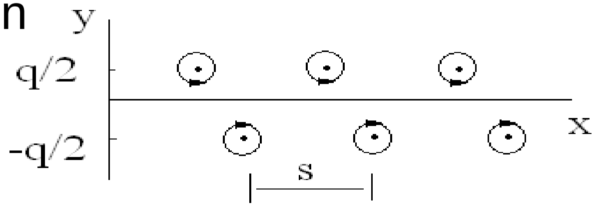


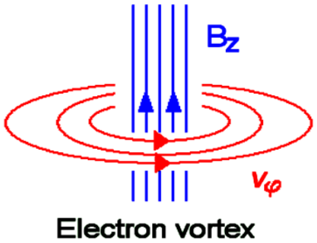


SVB, T.Esirkepov, M.Lontano, F.Pegoraro,A.Pukhov, Phys. Rev. Letts. 76, 3562 (1996).

# Interacting Point Vortices

As we know $\nabla\times(\mathbf{p}-e\mathbf{A}/c)$ is frozen:

$$(\partial_t+\mathbf{e}_z\times\nabla B\cdot\nabla)(\Delta B-B)=0$$

Discret vortices are described by equation $\Omega=\Delta B-B=\sum_j\Gamma_j\delta(\mathbf{r}-\mathbf{r}_j(t))$

its solution gives for the magnetic field $B=\sum_j B_j(\mathbf{r},\mathbf{r}_j(t))=-\sum_j\frac{\Gamma_j}{2\pi}K_0(|\mathbf{r}-\mathbf{r}_j(t)|)$

and the velocity of j-th vortex is

$$\frac{d\mathbf{r}_j}{dt}=\mathbf{e}_z\times\nabla\sum_{k\neq j}B_k(\mathbf{r}_j(t),\mathbf{r}_k(t)) \Longleftrightarrow \begin{cases}\dfrac{dx_j}{dt}=\dfrac{1}{2\pi}\sum_{k\neq j}\Gamma_k\dfrac{y_k-y_j}{|\mathbf{r}_j(t)-\mathbf{r}_k(t)|}K_1(|\mathbf{r}_j(t)-\mathbf{r}_k(t)|)\\[2ex]\dfrac{dy_j}{dt}=\dfrac{1}{2\pi}\sum_{k\neq j}\Gamma_k\dfrac{x_j-x_k}{|\mathbf{r}_j(t)-\mathbf{r}_k(t)|}K_1(|\mathbf{r}_j(t)-\mathbf{r}_k(t)|)\end{cases}$$

The Hamilton equations

# Stability Domain

Antisymmetric vortex row

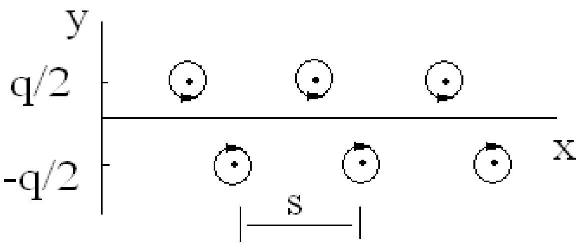


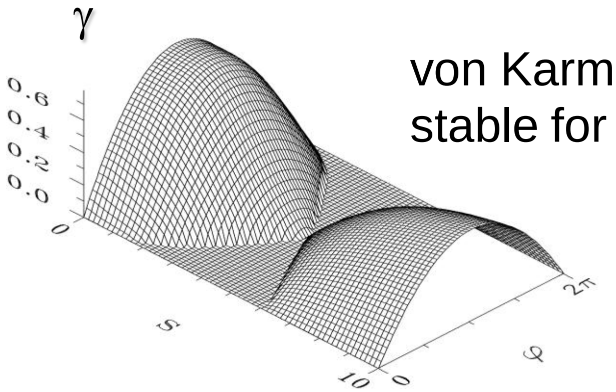


von Karman row is stable for q/s=0.281

Growth rate vs q and s for the H-M vortex row

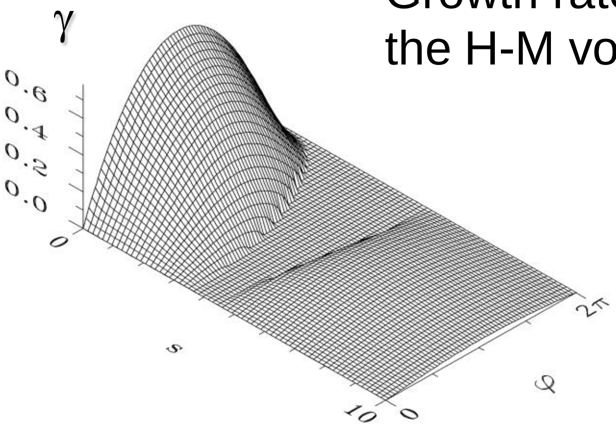


Lyapunov stability in the stability domain was proved

# 4. Relativistic Rotator

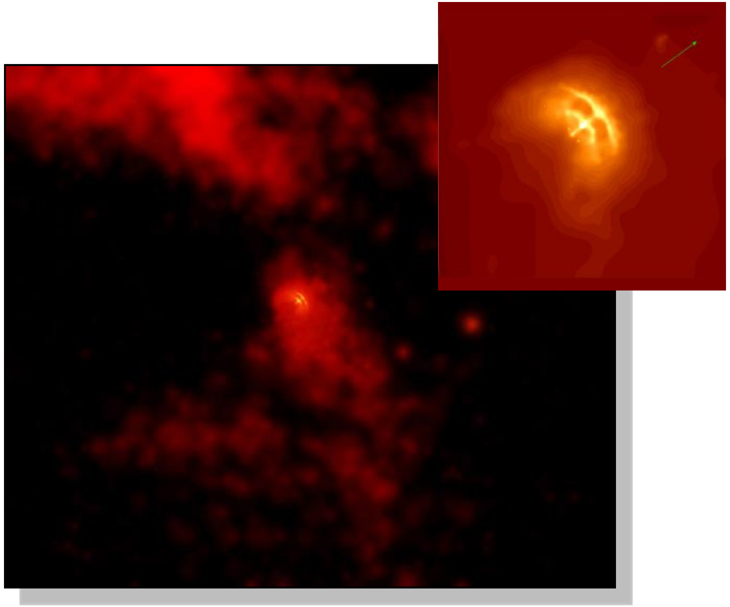

# PeV γ from Crab Nebula

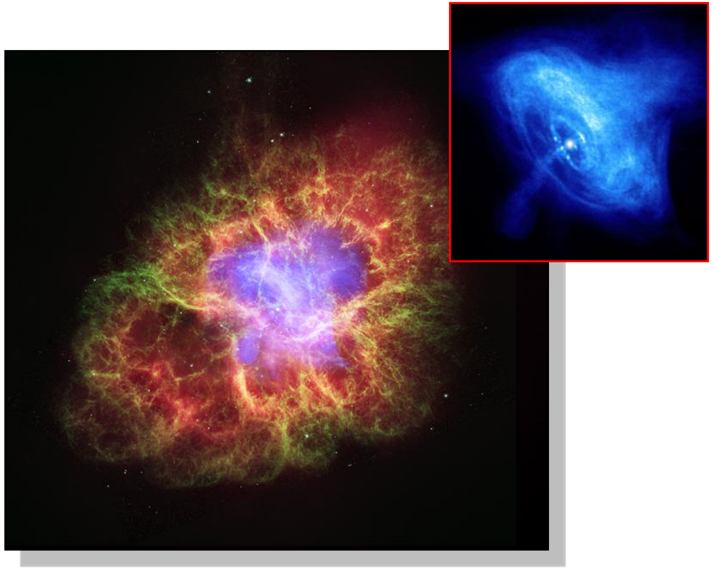

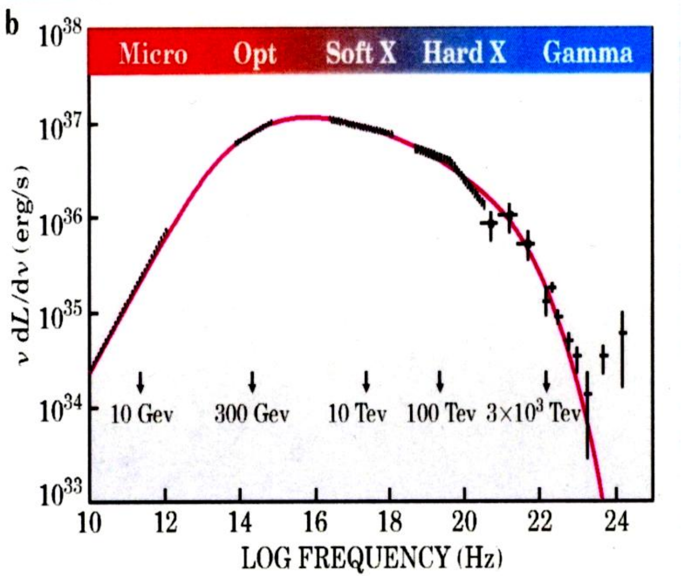


The Crab Pulsar, lies at the center of the Crab Nebula. The picture combines optical data (red) from the Hubble Space Telescope and x-ray images (blue) from the Chandra Observatory. The pulsar powers the x-ray and optical emission, accelerating charged particles and producing the x-rays.

# ON THE PULSAR EMISSION MECHANISMS

1975

*V. L. Ginzburg*
P. N. Lebedev Physical Institute, Academy of Sciences of the USSR, Moscow, USSR

*V. V. Zheleznyakov*
Radio-Physical Institute, Gorkii, USSR

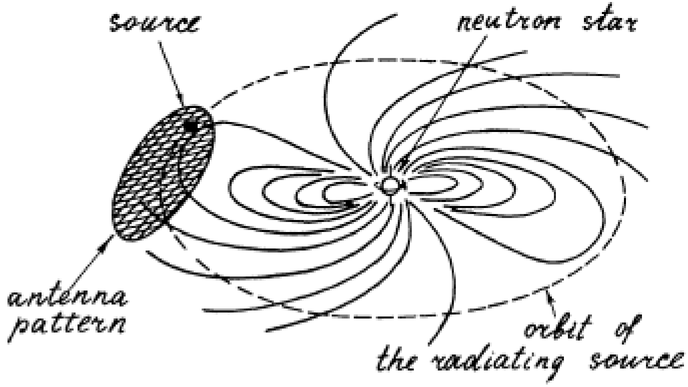


*Figure 2* Schematic pulsar model.

# Relativistic EM Soliton

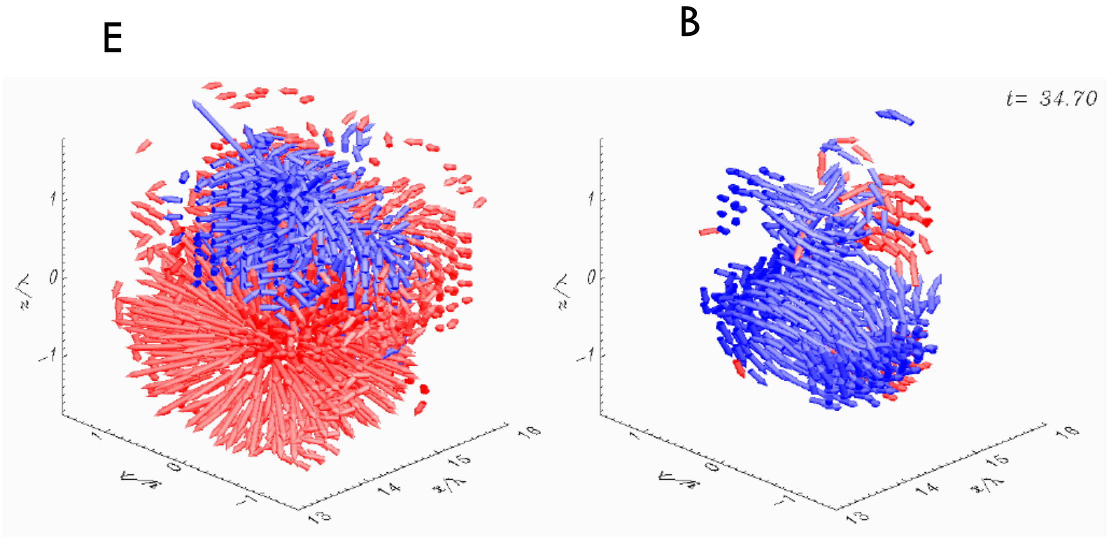


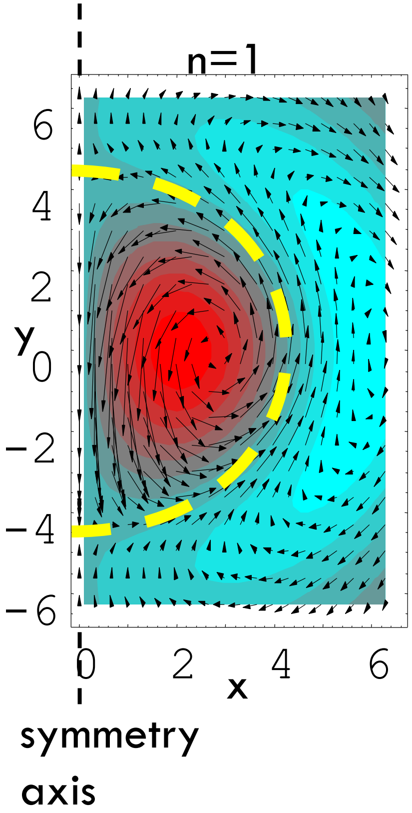


E.M. field in a spherical resonator

T.Esirkepov, SVB, K.Nishihara, F.Pegoraro, 2003

# Circularly Polarized Soliton (3D PIC)

$B_z(x,y)$

$n_e(x,y)$

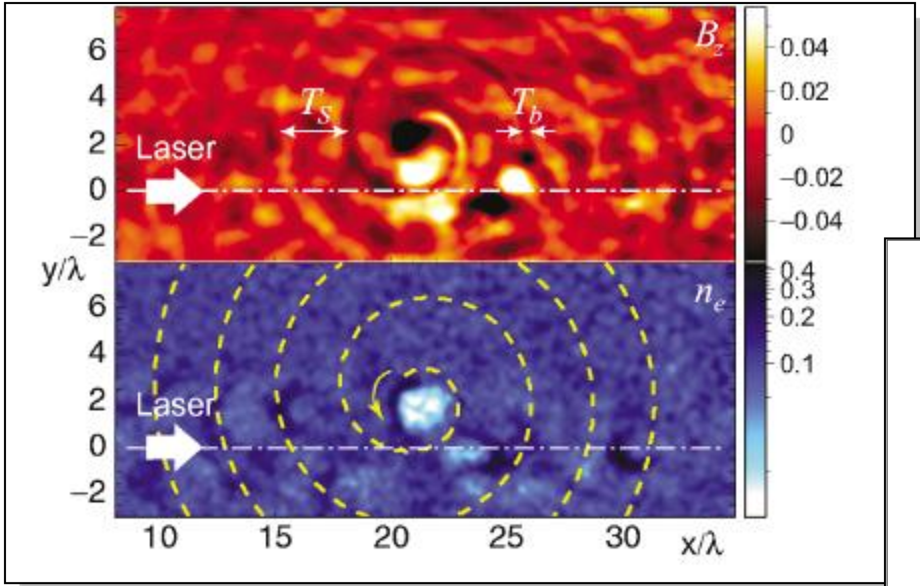


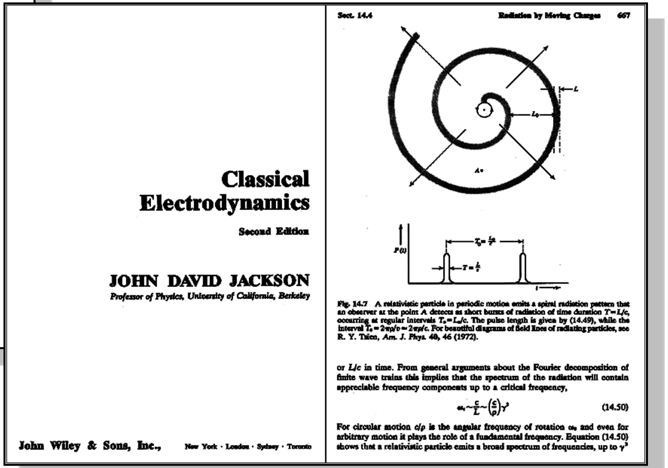
Classical Electrodynamics

Second Edition

JOHN DAVID JACKSON

Professor of Physics, University of California, Berkeley

John Wiley & Sons, Inc., New York · London · Sydney · Toronto

Sect. 14.4 Radiation by Moving Charges 667

Fig. 14.7 A relativistic particle in periodic motion emits a spiral radiation pattern that an observer at the point A detects as short bursts of radiation of time duration $T=L/c$, occurring at regular intervals $T_0=L_0/c$. The pulse length is given by (14.49), while the interval $T_0=2\pi\rho/v\approx 2\pi\rho/c$. For beautiful diagrams of field lines of radiating particles, see R. Y. Tsien, *Am. J. Phys.* 40, 46 (1972).

or $L/c$ in time. From general arguments about the Fourier decomposition of finite wave trains this implies that the spectrum of the radiation will contain appreciable frequency components up to a critical frequency,

$$\omega_c \sim \frac{c}{L} \sim \left(\frac{c}{\rho}\right)\gamma^3 \qquad (14.50)$$

For circular motion $c/\rho$ is the angular frequency of rotation $\omega_0$ and even for arbitrary motion it plays the role of a fundamental frequency. Equation (14.50) shows that a relativistic particle emits a broad spectrum of frequencies, up to $\gamma^3$

T.Esirkepov, SVB, K.Nishihara, T.Tajima, PRL (2004)

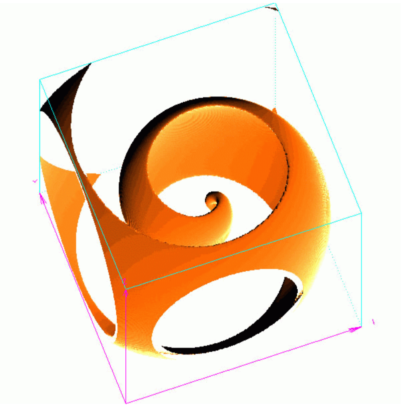

E.M. field energy density

Energy loss by radiation

$$-\frac{d\mathcal{E}}{dt}=\frac{2e^2}{3c}N^2\omega_0^2\gamma^2\left(\gamma^2-1\right)$$

Frequency distribution of the total energy emitted by coherently rotating electrons

$$\frac{dI}{d\omega}=\sqrt{3}N^2\gamma\frac{e^2}{c}\frac{2\omega}{3\gamma^3\omega_0}\int_{\frac{2\omega}{3\gamma^3\omega_0}}^{\infty}K_{5/3}(\xi)\,d\xi$$

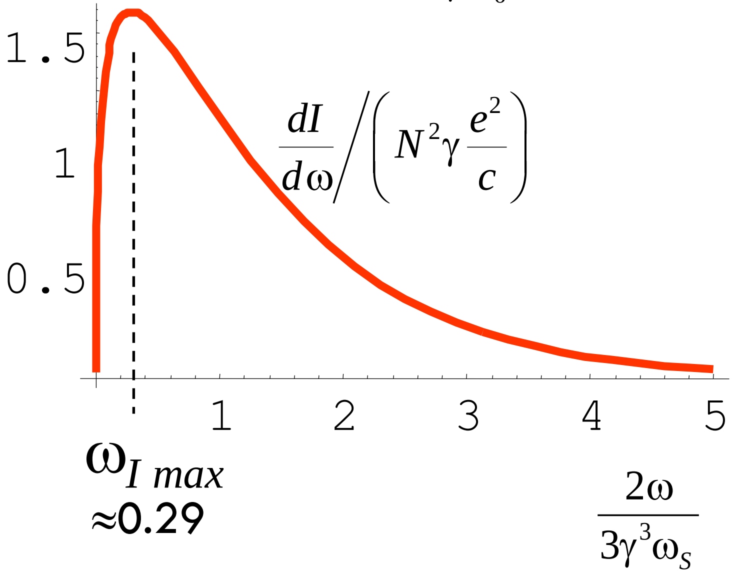

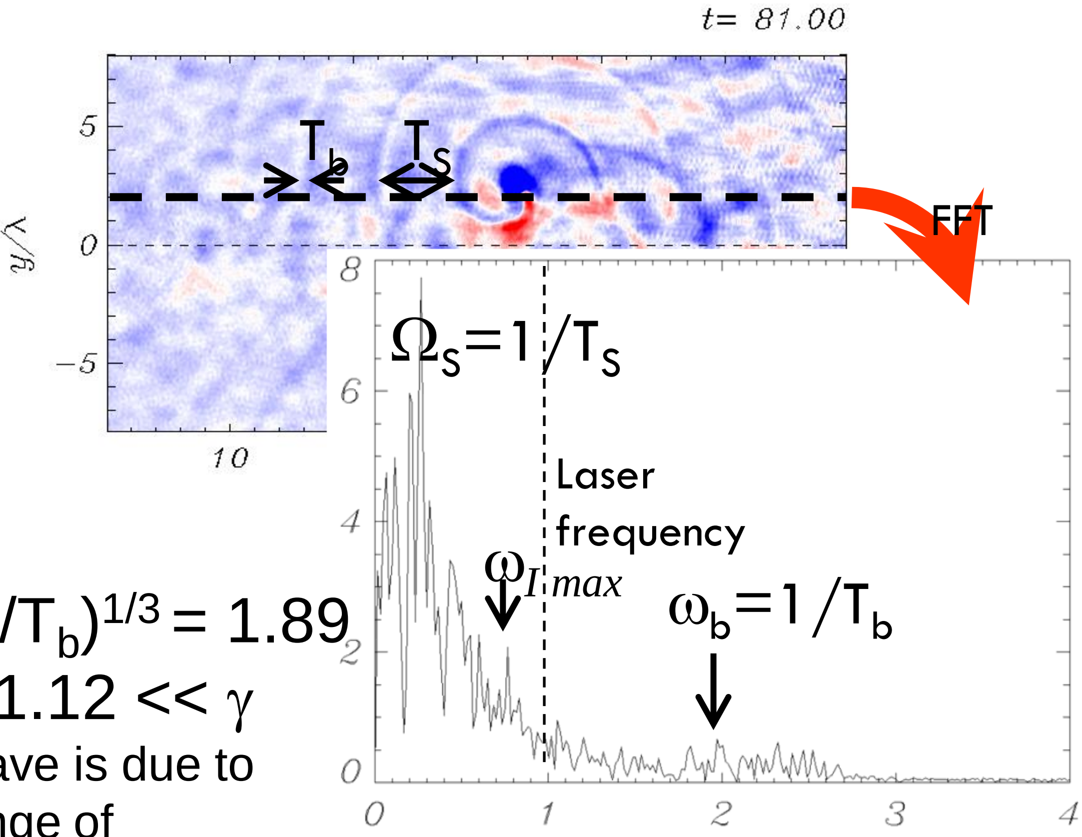


$\gamma \approx (T_S/T_b)^{1/3} = 1.89$

$\gamma_{e\ max} = 1.12 << \gamma$

Spiral wave is due to fast change of electric charge density!

**The solitons as the relativistic rotators can model the pulsar radiation under the earth laboratory conditions**

# 5. Flying Mirror
# for Femto-, Atto-, …
# Super Strong Field Science

**Kagami** 鏡

(“mirror” in Japanese)

# Flying Mirror Concept

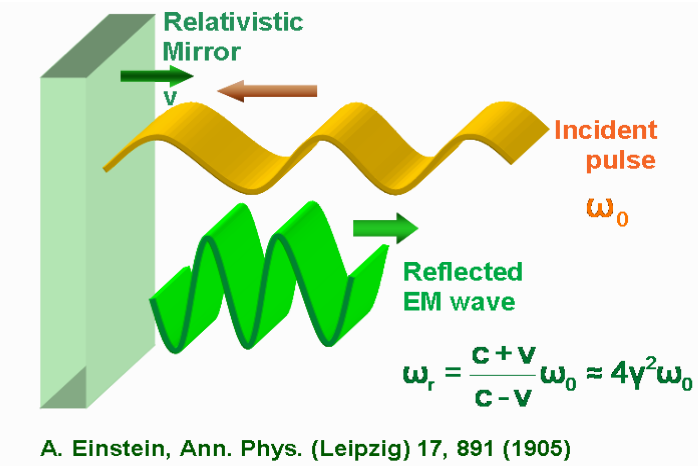


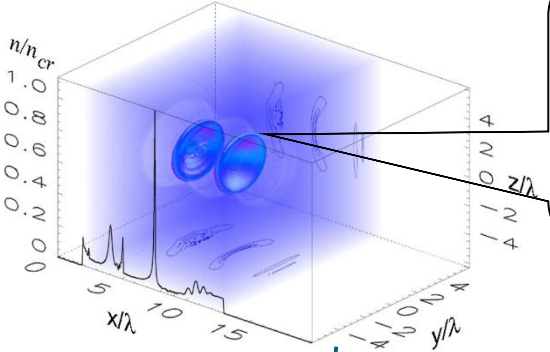


paraboloidal relativistic mirrors formed by the wake wave left behind the laser driver pulse

laser pulses

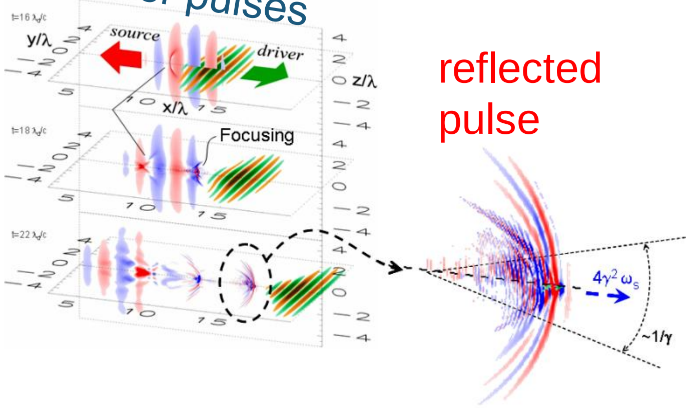


reflected pulse

**Frequency up-shifting and intensification of the light reflected at the relativistic mirror**

S. Bulanov, T. Esirkepov, T. Tajima, Phys. Rev. Lett. 91, 085001 (2003)

# Laser Energy & Power to Achieve the Schwinger Field

**The driver and source must carry 10 kJ and 30 J, respectively**

**Reflected intensity can approach the Schwinger limit** $I_{QED} = 10^{29} W / cm^2$

$$E_{QED} = \frac{m_e^2 c^3}{e\hbar}$$

**It becomes possible to investigate such the fundamental problems of nowadays physics, as e.g. the electron-positron pair creation in vacuum and the photon-photon scattering**

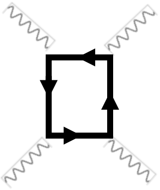

$$\mathcal{L} = \frac{1}{16\pi} F_{\alpha\beta}F^{\alpha\beta} - \frac{\kappa}{64\pi}\left[5\ F_{\alpha\beta}F^{\alpha\beta}\ ^2 - 14 F_{\alpha\beta}F^{\beta\gamma}F_{\gamma\delta}F^{\delta\mu}\right]$$

**The critical power for nonlinear vacuum effects is**

$$\mathcal{P}_{cr} = \frac{45\pi^2}{\alpha}\frac{cE_{QED}^2\lambda^2}{4\pi}$$

$$\mathcal{P}_{cr} \approx 2.5 \times 10^{24} W$$

**Light compression and focusing with the FLYING MIRRORS yields** $\mathcal{P} = \mathcal{P}_0 \gamma_{ph}$

**for** $\lambda_0 = 1\mu m$ $\lambda = \lambda_0 / 4\gamma_{ph}^2$ **with** $\gamma_{ph} \approx 30$ **the driver power** **$P_{cr}$=10 PW**

# Proof of Principle Experiment

**In our experiments, narrow band XUV generation was demonstrated**

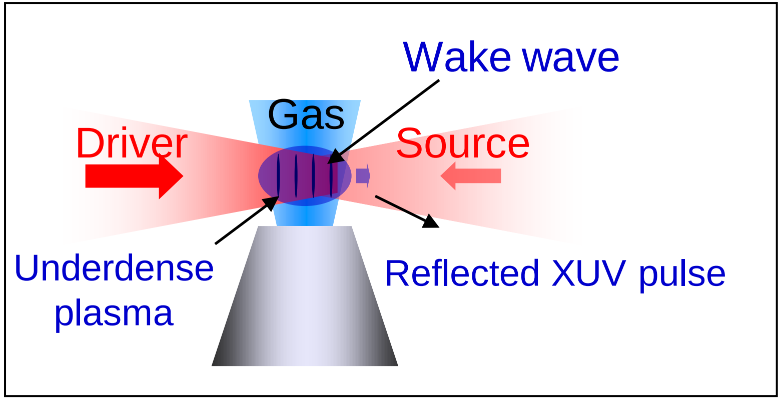


Gas jet profile

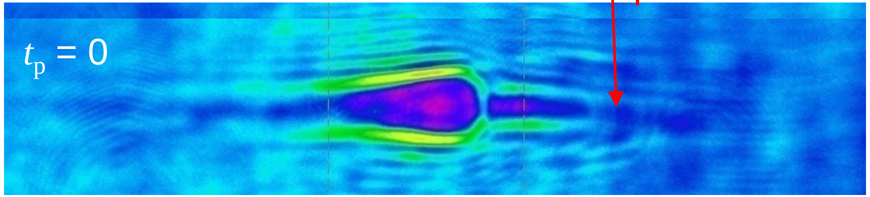


Detected signals

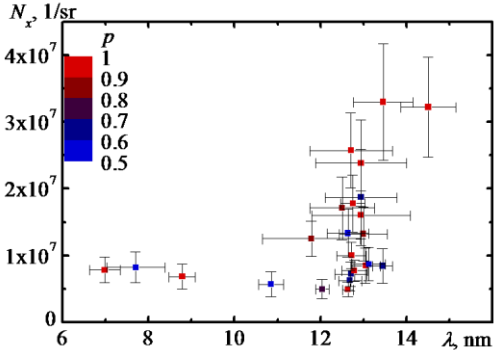


**Frequency multiplication**

$$\frac{\omega_r}{\omega_s} = 55\ldots114$$

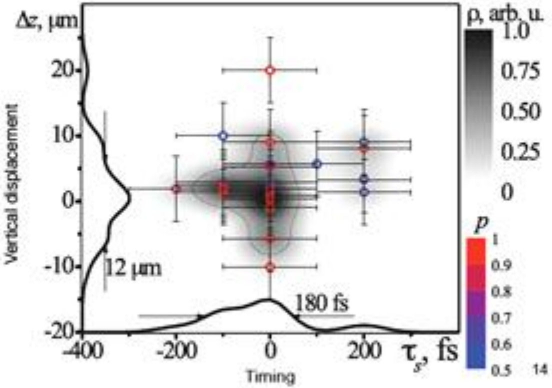


**M. Kando, et al., Phys. Rev. Lett. 99, 135001 (2007);**
**A. Pirozhkov, et al., Phys. Plasmas 14, 123106 (2007)**

# Flying Mirror in the Head-On Collision Experiment

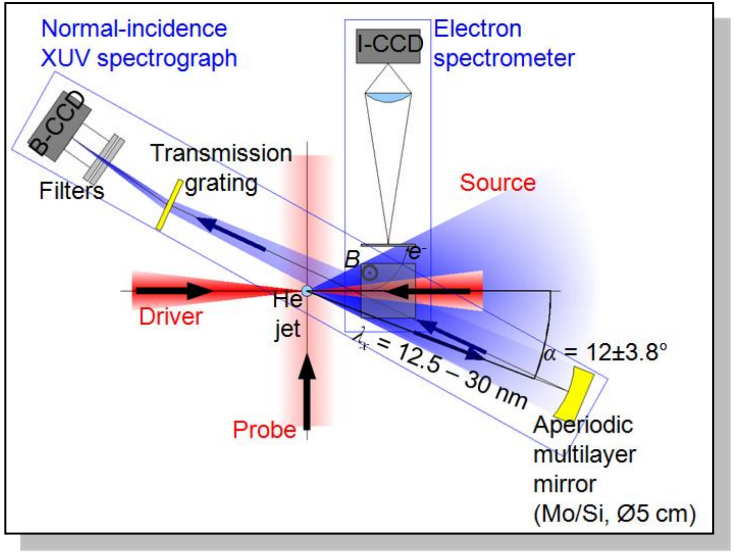


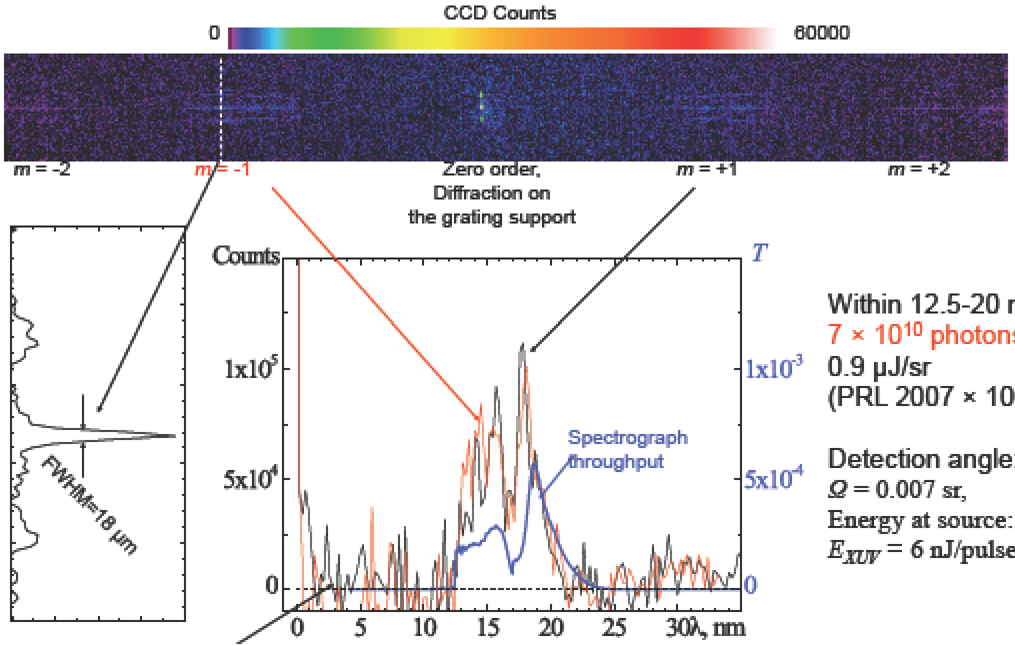


**noise**

Within 12.5-20 nm:
$7 \times 10^{10}$ photons/sr
0.9 μJ/sr
(PRL 2007 × 1000)

Detection angle:
$\Omega = 0.007$ sr,
Energy at source:
$E_{XUV} = 6$ nJ/pulse

**Two head-on colliding laser pulses**

# 6. Overdense Accelerating Mirror

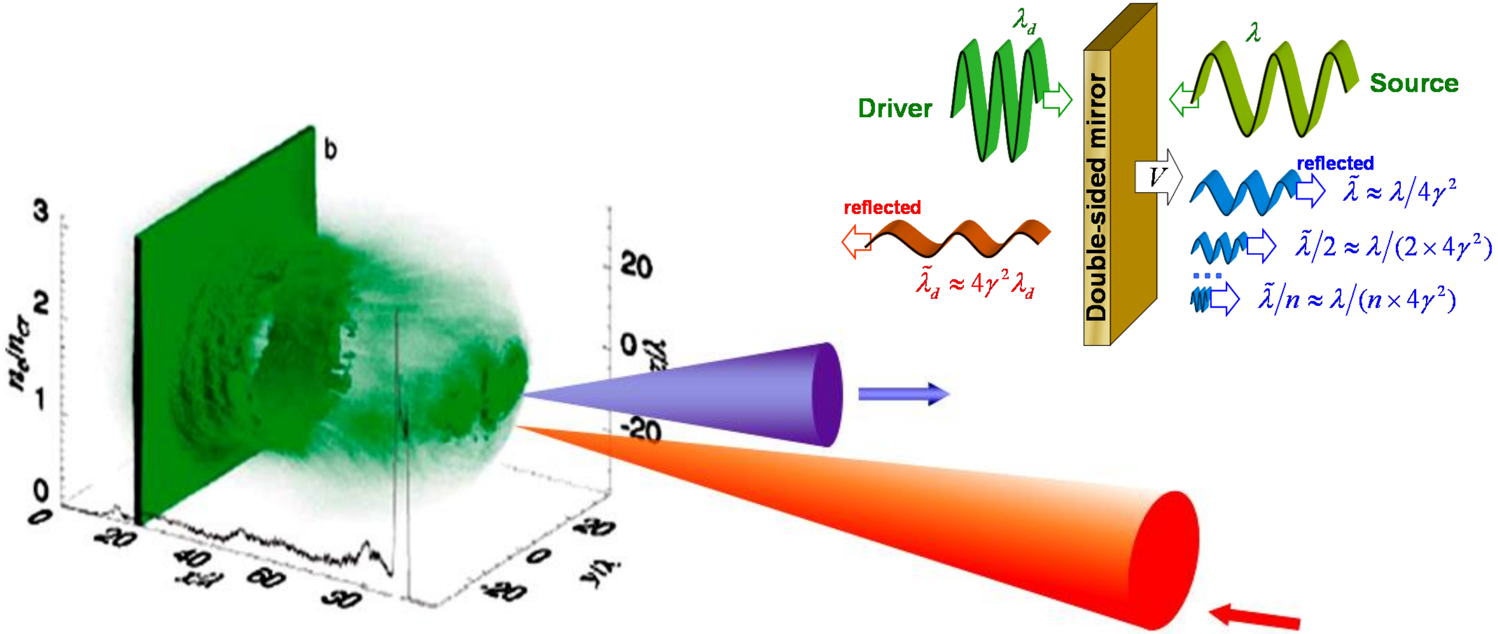


T.Esirkepov, et al. Phys. Rev. Lett. (2009)

# Accelerating Double-Sided Mirror: Boosted HOH

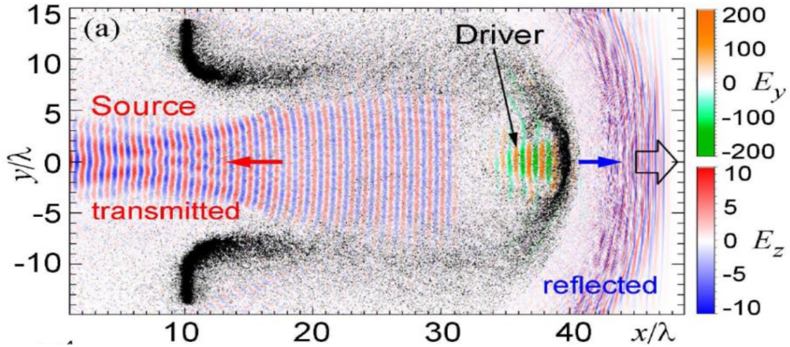


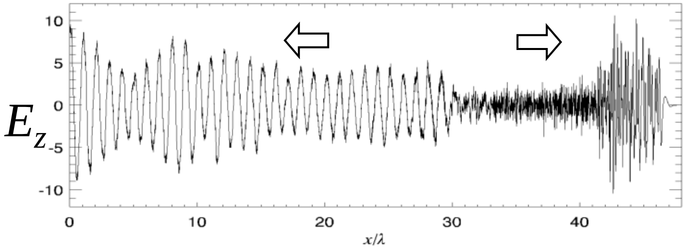


Reflected cycles

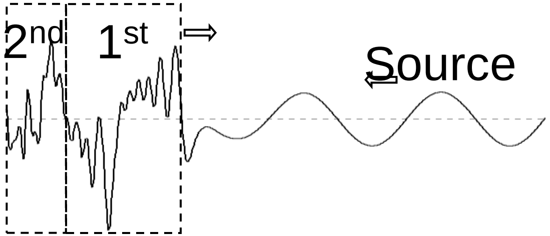


Field along $x$-axis

Spectrum at fixed time

$$I_\omega(t) = \int_{-\infty}^{+\infty} E_z(\tau) e^{-i\tau\omega - c^2(\tau - t)^2/\lambda^2} d\tau$$

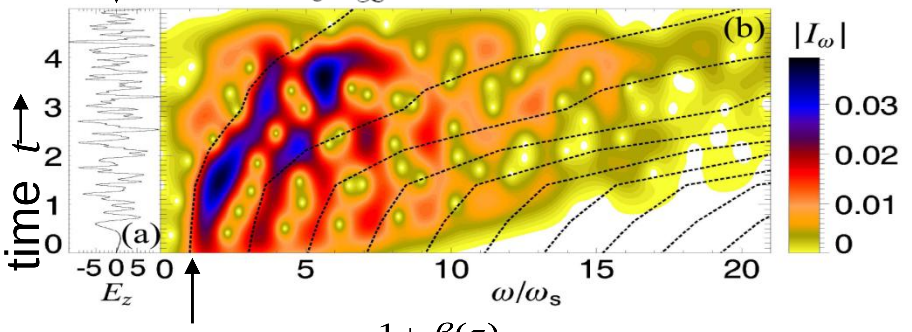


**Dashed curves:** $\frac{1+\beta(\tau)}{1-\beta(\tau)} \omega_0 \times (2n-1), \ \ n = 1, 2, 3 \ldots$

$\tau$ – time of emission

time of detection: $t = \tau - \int_0^\tau \beta(\tau) d\tau$

**Reflected light structure:**

- Fundamental mode $\times 4\gamma^2$
- High harmonics $\times 4\gamma^2$
- Shift due to acceleration

# 7. Applications

**Such X-ray sources are expected for applications and for fundamental science.**

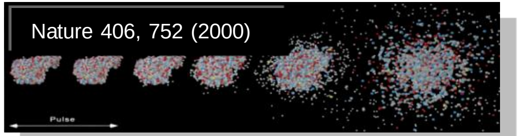


**a) biology and medicine - single-shot X-ray imaging in a 'water window' or shorter wavelength range.**

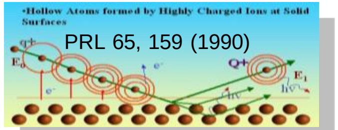


**b) atomic physics and spectroscopy – the multi-photon ionization & high Z hollow atoms (and ions).**

**c) probing relativistic plasmas, for the nonlinear wave theory**

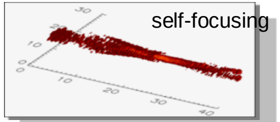



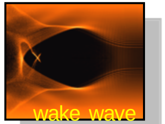


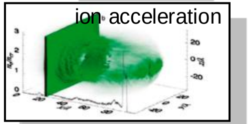


**& for charged particle acceleration**

**d) novel regimes of soft X ray - matter interaction: dominant radiation friction & quantum physics cooperative phenomena.**

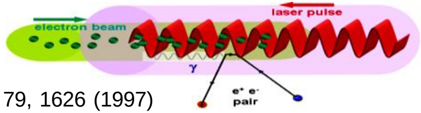


PRL 79, 1626 (1997)

# High Field Science

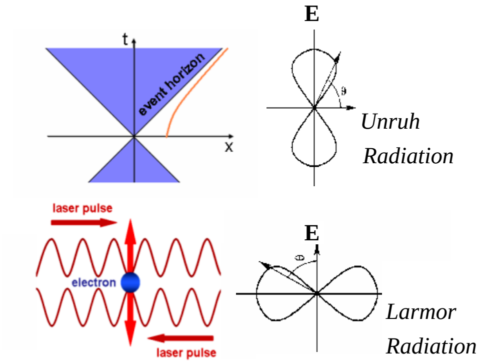


Unruh radiation (Chen&Tajima (1999))


Birefringent e.m. vacuum (Rosanov (1993))

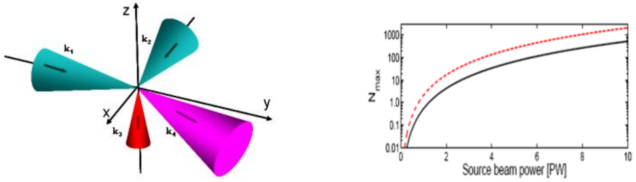


4-wave mixing (Lundström et al (2006))

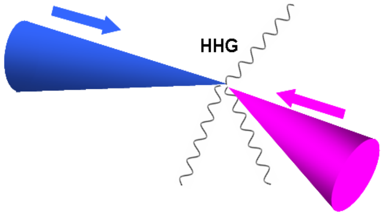


Higher harmonic generation through quantum vacuum interaction (Fedotov & Narozhny (2006); Di Piazza, Keitel)

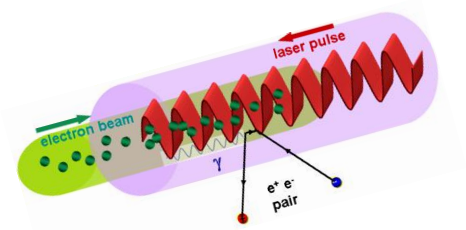


Electron-positron pair production in the laser interaction with the electron beam: $e^- + n\gamma \rightarrow \gamma,\ \gamma + n\gamma' \rightarrow e^+ + e^-$
Bula et al (1996); Burke et al (1997)

# Compact Coherent Ultrafast X-Ray Source

| X-ray source | Wavelength | Pulse Duration | Pulse Energy | Mono-chromaticity (Δλ/λ) | Coherence |
|---|---|---|---|---|---|
| XFEL (DESY) | 13.8 nm | 50 fs | 100 μJ | $10^{-3}$ | spatial good |
| Plasma XRL | 13.9 nm | 7 ps | 10 μJ | $10^{-4}$ | spatial good |
| Laser plasma | wide spectrum 1 nm – 40 nm | 1 ps – 1 ns | 10 μJ | $10^{-2}$ – $10^{-3}$ | No |
| HHG | 5 – 200 nm | 100 attosec | 1 μJ | $10^{-2}$ – $10^{-3}$ | spatial and temporal good |
| Flying Mirror | 0.1 – 20 nm | < 1 fs | 1 mJ | $10^{-2}$ – $10^{-4}$ | spatial and temporal good |

**Predicted by the FM theory parameters of the x-ray pulse compared with the parameters of high power x-ray generated by other sources**

## Brightness

$$B = 2\times10^{28}\left(\frac{\mathcal{E}_{las}}{1\mathrm{J}}\right)\sqrt{\frac{1\mathrm{KeV}}{\hbar\omega_\gamma}}\frac{1}{\mathrm{mm}^2\,\mathrm{mrad}^2\,0.1\%\,\mathrm{bandwidth}}$$

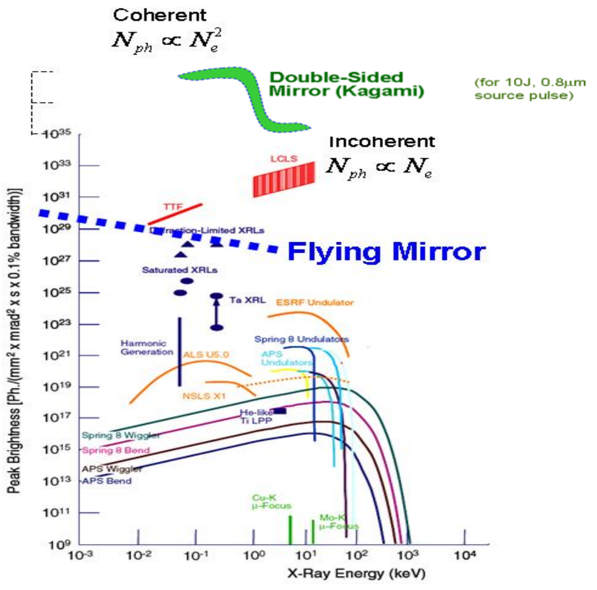


Peak brightness of various light sources

# 8. Conclusion

a) Ultra Short Pulse Laser – Matter Interaction has entered the Ultrarelativistic Regime. By this it has opened a new field of Relativistic Laboratory Astrophysics

b) Laser Piston+Flying Mirror+Oscillating Mirror will provide in a nearest future the instruments for nonlinear vacuum probing and for studying other fundamental problems